# Effects of vegetation canopy density and bank angle on near-bank patterns of turbulence and Reynolds stresses

Nicole M. Czarnomski[1], Desireé D. Tullos[2], Robert E. Thomas[3], and Andrew Simon[4]

[1]Watershed Sciences Department, Utah State University, 5210 Old Main Hill, Logan, UT 84322; PH (435) 797-2459; FAX (435) 797-1871; email: nicole.czarnomski@usu.edu

[2]Department of Biological and Ecological Engineering, Oregon State University, Corvallis, OR 97331; PH (541) 737-2038; FAX (541) 737-2082; email: desiree.tullos@oregonstate.edu

[3]Department of Geography, University of Hull, Cottingham Road, Hull, HU6 7RX. UK; PH +44 (0)1482 465355; FAX +44 (0)1482 466340; email: r.e.thomas02@members.leeds.ac.uk

[4]CardnoENTRIX, 1223 Jackson Avenue East, Suite 301, Oxford, MS 38655; PH (662) 236-6983; FAX (662) 281-9942; email: andrew.simon@cardno.com

## Abstract

Vegetation growing on the surface of a streambank has been shown to alter the shear stresses applied to the boundary, but basic questions remain regarding the influence of vegetation and streambank configurations on near-bank hydraulics. In the present study, Froude-scaled flume experiments were used to investigate how changes in vegetation density (ratio of frontal area to channel area, including both stems and leaves) and bank surface angle influence near-bank turbulence intensities ($RMS_{u,v,w}$) and Reynolds stresses ($\tau_{uv}$ and $\tau_{uw}$) estimated using velocities obtained with an acoustic Doppler velocimeter positioned beneath the canopy. Results illustrate how, with increasing vegetation density, turbulence intensities and Reynolds stresses decreased along the sloped bank surface but increased at the base of the slope and within the main channel. The steeper bank angle resulted in greater vertical stresses on the bank surface than the shallower angle, but lateral momentum exchange was larger than vertical exchange along the base of the slope, regardless of bank angle. Leaves were an important influence on near-bank turbulence intensities and Reynolds stresses, while the influence of bank slope was small relative to the influence of vegetation density.

## Introduction

Vegetation on the base of streambanks may deflect flow and reduce near-bank velocities and shear stresses, but may also induce turbulence, elevate shear stresses and promote localized scour along the base of the bank surface (Wilkerson 2007; Yang et al. 2007; Gorrick 2009; Hopkinson and Wynn 2009). Vegetation also generates turbulence in the vertical plane at the interface between the canopy and the free-stream (Yang et al. 2007; White and Nepf 2008; Hopkinson and Wynn 2009; Zong and Nepf 2010). Shear layers form at interfaces between vegetated patches and the free-stream, spawning coherent vortices and eddies (Nepf 1999; White and Nepf 2008; Zong and Nepf 2010). Although it has been found in some cases (e.g., Wilkerson 2007; Hopkinson and Wynn 2009) that plant-flow interactions are similar on banks and floodplains, and that turbulence levels on inclined non-vegetated and sparsely-vegetated streambanks are sometimes similar (Hopkinson and Wynn 2009), other studies (Nepf 1999; McBride et al. 2007) document elevated turbulence levels within sparsely-treed floodplains relative to the non-vegetated case. This apparent dichotomy suggests that site-specific conditions, such as the angle of the bank face and/or bank toe, may influence the relationship between vegetation and channel hydraulics (McBride et al. 2007; Wilkerson 2007). Therefore, the objective of the present study is to use a Froude-scaled flume experiment to characterize the interacting influences of bank angle and vegetation density, defined as the ratio of plant frontal area (the area of submerged leaves and stems in a vertical plane perpendicular to the channel centerline) to flow area, on near-bank patterns of shear stress and turbulence.

## Methods

Experiments were conducted in a 6.0 m × 0.6 m × 0.6 m recirculating flume set at a fixed slope of 0.01 m $m^{-1}$. At the inlet, a rock-filled baffle box and 0.30 m-long, 0.02 m-diameter tubes (flow straighteners) were used to dampen turbulence and provide parallel streamlines. To simulate a sloping bank surface along one side of the flume, a 4.88 m-long insert, inclined at either 15° or 30° from the horizontal, was installed immediately downstream of the flow straighteners. Stands of artificial vegetation of two different stem densities (defined as the number of stems per square meter of bank surface) and two different leaf scenarios (“leaved” and “leafless”; the prefix L is used throughout the text to denote leaved cases; e.g., $LD_{lo}$, $LD_{hi}$) were installed in a staggered pattern on the bank surface (Figure 1). Stems for the artificial plants were constructed using acrylic rods; ten 28-gauge wire “branches” with 25 × 35 mm flexible “leaves” made of contact paper were affixed to the rods in a pattern similar to Wilson et al. (2006a) and commencing 60 mm above the base of the stem. Other than the vegetative elements, the boundaries of the flume were smooth: the flume walls were constructed of lacquered marine plywood. Flow depth was controlled by a weir at the outlet, creating a gradually-varied, highly-subcritical (Table 1), and fully turbulent ($15644 \leq Re \leq 16095$) flow field. Water depths were always less than the height of the plants and hence the plants were emergent.

Flume geometry was Froude-scaled from the Goodwin Creek bendway site in North Mississippi (Langendoen and Simon 2008; Simon et al. 2000; Simon and Collison 2002; Wood et al. 2001) to establish both geometric and kinematic similitude (Table 1). Bank slope lengths and angles were computed for repeat surveys at eleven cross-sections at Goodwin Creek, and two (cross-sections 5 and 6; Table 2) were selected for representation in the flume. The 15° and 30° bank angles in our physical model approximate the $10^{th}$ and $90^{th}$ percentiles observed in the prototype, respectively. Owing to limitations imposed by the dimensions of the flume, the selected length scales were computed using the ratios between the model slope lengths (0.41 and 0.46 m, respectively) and the $16^{th}$ percentile slope length (~2.0 m), rather than the median slope length (3.3 m) of the prototype bank. This scaling approach yielded mean Froude scaling factors of 4.88 and 4.35 for the 15° and 30° bank surface, respectively.

Features (i.e., stem diameter, stem density, frontal area and flexural rigidity) of the artificial vegetation were also scaled (Table 1). Vegetation models were based on willow and cottonwood yearlings up to 2 m-tall and 20 mm-diameter, which are commonly found on periodically-inundated bank surfaces in densities of ~10 to 30 stems $m^{-2}$ (Wilson et al. 2006b). Thus, applying Froude scaling, artificial plants were constructed using 450 mm-long, 4.54 mm-diameter acrylic rods and arranged with stem densities of 202 and 615 stems $m^{-2}$, respectively, in a 3 m-long array, beginning immediately downstream of the flow straighteners. The flexural rigidity ($J$) of stems was also Froude-scaled (Table 1), based on field data collected during the present study (see Czarnomski 2010 for further details) and values reported by others (Niklas 1992; Freeman et al. 2000; Wilson et al. 2003). Note that Reynolds number similarity was necessarily relaxed (Yalin 1971).

*Near-bed velocity measurements*

Near-bed velocities were measured at seven cross-sections spaced 0.055 m apart at approximately 5 mm above the bed. In order to limit the influence of conditions imposed at the inlet and outlet, cross-sections were located 1.84 – 2.23 m downstream from the flow straighteners. Velocities were measured at 25 Hz for 300 seconds with a downward-looking 10 MHz Nortek acoustic Doppler velocimeter (ADV) that was aligned with the $z$-axis (see Figure 1 for a definition of the Cartesian coordinate system employed). Sampling frequency was selected assuming a Strouhal number of 0.21 (e.g., Schlichting 1968), estimating the likely eddy shedding frequency caused by model stems (9.1 – 12.3 Hz) and then considering the Nyquist sampling theorem. Sampling duration was selected after analysis of the cumulative velocity variance associated with different sampling windows (e.g., Sukhodolov and Rhoads 2001). The sampling volume of the ADV had a diameter of 6 mm and a volume of 254 $mm^3$, thus capturing turbulent eddies that were approximately as small as the stem diameter. Boundary measurements were made at fixed $x$-$y$ coordinates for each of the seven cross-sections and were generally located 0.01- 0.03 m away from the nearest stem. However, if a velocity sampling location fell within 0.01 m of a stem, that stem was temporarily removed to permit data acquisition. ADV data with average correlation coefficients < 0.6 and signal-to-noise ratios < 0.15 dB were removed and the remaining data were despiked using the phase-space threshold algorithm (Goring and Nikora 2002) within WinADV version 2.027 (Wahl 2009).

*Analysis of velocity measurements*

Using near-bed velocities measured at the cross-section 2.0 m from the beginning of the vegetation, we computed the root mean square ($RMS$) difference between the instantaneous velocities ($u$, $v$, and $w$) in the streamwise ($x$), lateral ($y$), and vertical ($z$) directions and their respective time-averages ($\bar{u}$, $\bar{v}$, and $\bar{w}$) to represent turbulence intensity (Hinze 1975) and to provide an indication of where shear stresses are highest (Biron et al. 2004; Hopkinson and Wynne 2009). Computed values of $RMS$ were normalized by the cross-sectional mean velocity ($U$) to facilitate comparison of the three components and to illustrate the magnitude of turbulent fluctuations relative to the mean flow.

Local estimates of lateral and vertical Reynolds stresses ($\tau_{uv}$ and $\tau_{uw}$, respectively) were used as proxies for applied shear stress (e.g., Biron et al. 2004) and to quantify the magnitude and direction of turbulent fluctuations that represent momentum exchange across a given plane

(Robert 2003). $\tau_{uv}$ and $\tau_{uw}$ were estimated for all sampling points using $\tau_{uv} = -\rho\overline{u'v'}$ and $\tau_{uw} = -\rho\overline{u'w'}$, respectively, where primes denote fluctuations about the time averaged velocities.

## Results

### *Relative turbulence intensity (RMS/U)*

The presence of vegetation on the bank surface generally increased *RMS/U* at the base of the bank slope and immediately adjacent to the bank (Figure 2). For example, at the base of the bank slope, *RMS/U* increased by 120 – 650% over the non-vegetated scenario for $LD_{lo}$, $LD_{hi}$ and $D_{hi}$. At this location, values of *RMS/U* were also much higher for leaved than for leafless vegetation. For example, relative to the non-vegetated case, at the base of the 15° slope, $RMS_u/U$, $RMS_v/U$, and $RMS_w/U$ increased by 60 – 150% during leafless vegetated runs, but by 220 – 320% during leaved runs (Figure 2). A similar result was true for the 30° bank: at the base of the bank slope, *RMS/U* increased by 140 – 220% during leafless runs and by 350 – 650% during leaved runs (Figure 2).

Streamwise relative turbulence intensity ($RMS_u/U$) ranged from 85 – 160% of the lateral relative turbulence intensity ($RMS_v/U$), and from 210 – 490% of the vertical relative turbulence intensity ($RMS_w/U$). The differences in intensity were similar for the 15° and 30° bank slopes, although the peak magnitude of $RMS_u/U$ on the 30° bank was up to 30% larger than $RMS_u/U$ on the 15° bank and $RMS_v/U$ was 100% larger on the 30° bank than $RMS_v/U$ on the 15° bank.

### *Reynolds stresses*

Spatial patterns of near-bed values of $\tau_{uw}$ and $\tau_{uv}$ were similar to patterns of *RMS/U*, where values were generally positive and increases in stress were observed with increasing plant density. Without vegetation, $\tau_{uw}$ values were generally positive (0 – 0.05 Pa) and were mostly distributed uniformly throughout the cross-section (Figure 3). Once vegetation was introduced, values of $\tau_{uw}$ were positive within the main channel, with a local maximum near the center of the main channel, and negative on the bank surface, with a local minimum near the base of the slope (Figure 3). $\tau_{uw}$ was up to an order of magnitude lower for the 15° bank than the 30° bank, and the magnitude of $\tau_{uw}$ at the stationary points (e.g. maxima, minima) increased with increasing vegetation density (Figure 3). Similar patterns were observed for $\tau_{uv}$, where increasing vegetation led to higher values of $\tau_{uv}$, indicating increases in lateral momentum exchange across the base of the slope. However, the magnitude of $\tau_{uv}$ across the slope base was similar along the 15° and 30° banks (Figure 4).

The dominant orientation of stresses and momentum exchanges was more variable on the 15° bank than the 30° bank (Figures 3 and 4). For the 30° bank, lateral momentum exchange was the primary stress found throughout the channel when vegetation was not present. With high density vegetation along the 30° bank, the primary stress on the bank surface was $\tau_{uw}$, while $\tau_{uv}$ was higher along the base of the slope and in the main channel. For the 15° bank, $\tau_{uv}$ was dominant at the base of the slope when no vegetation was present, but neither $\tau_{uv}$ nor $\tau_{uw}$ was consistently dominant when vegetation was present.

## Summary and Conclusions

This paper has presented results from an experimental study aimed at characterizing the influence of bank angle and vegetation density on near-bank patterns of shear stress and turbulence. The key findings of the study are:

1. Increasing bank angle caused increased turbulence intensities and Reynolds stresses at the base of the bank slope. However, on the bank slope itself, relative turbulence intensities and Reynolds stresses were insensitive to the angle of the bank;
2. Increasing vegetation density on the bank surface caused increased near-bed turbulence intensities and Reynolds stresses in the main channel and at the base of the slope. These increases were particularly evident along the base of the slope, supporting the findings of previous studies (e.g., Yang et al. 2007; Gorrick 2009; Hopkinson and Wynn 2009); and
3. Relative turbulence intensities and Reynolds stresses were higher for leaved than for leafless conditions. This result highlights the importance of including leaves or equivalent canopy roughness in both flume and numerical experiments and casts doubt on the results of studies that have not done so. The additional frontal area afforded by a canopy, and the hydraulic behavior of a canopy, cannot be replicated by merely increasing stem density, but instead requires the use of vegetative elements of a more realistic morphology (e.g., Yang et al. 2007; Hopkinson and Wynn 2009).

It is acknowledged that the strength of these conclusions may be reduced by the lack of uniform flow in our flume and we therefore encourage future studies to more carefully develop uniform flow conditions (Tracy and Lester 1961). Nonetheless, the results presented herein contribute to the growing knowledge (e.g., Nepf 1999; Wilson et al. 2003; McBride et al. 2007; Yang et al. 2007; Gorrick 2009; Hopkinson and Wynn 2009) of the influence of vegetation morphology and configuration on near-boundary hydraulics. Furthermore, they emphasize the need to consider the morphology of vegetation when assessing turbulence and stress within patches of vegetation, and to evaluate the timing of flood events relative to leaf-out when planting vegetation as a management strategy to deflect near-bank flows.

## Acknowledgements

Support for this research was provided by an NSF IGERT graduate fellowship (NSF award 0333257) in the Ecosystem Informatics IGERT program at Oregon State University and the USDA-ARS National Sedimentation Laboratory at Oxford, Mississippi. Cross-sections at the Goodwin Creek bendway site were surveyed by staff of the Watershed Physical Processes Research Unit of the USDA-ARS-NSL. We appreciate advice provided by Vincent Neary. We are also grateful for technical advice and review provided by Daniel Wren and technical assistance provided by Lee Patterson. This manuscript was greatly improved by the comments of four anonymous reviewers, the associate editor and the editor.

## References


Biron, P. M., Robson, C., Lapointe, M. F., and Gaskin, S. J. (2004). "Comparing different methods of bed shear stress estimates in simple and complex flow fields." *Earth Surface Processes and Landforms*, 29, 1403-1415.

Czarnomski, N. M. (2010). "Influence of vegetation on streambank hydraulics." Ph.D. thesis, Oregon State University, Corvallis, OR.

Freeman, G. E., Rahmeyer, W. H., and Copeland, R. R. (2000). "Determination of resistance due to shrubs and woody vegetation." ERDC/CHL Technical Report 00-25, US Army Corps of Engineers, Vicksburg, MS.

Goring, G. and Nikora, V. (2002). "Despiking acoustic Doppler velocimeter data." *Journal of Hydraulic Engineering, ASCE* 128(1), 117-126.

Gorrick, S. (2009). "Field and laboratory investigations on the effects of riparian vegetation on stream flow and sediment dynamics." *Proceedings of the 33rd IAHR Congress (CD-ROM)*, IAHR, Madrid, Spain, Session TS-11, Track KE, 8 pages.

Hinze, J.O. (1975). "Turbulence, 2nd edition." McGraw Hill, New York, NY.

Hopkinson, L., and Wynn, T. (2009). "Vegetation impacts on near bank flow." *Ecohydrology*, 2(4), 404-418.

Julien, P. Y. (2002). "River Mechanics." Cambridge University Press, New York, NY.

Langendoen, E. J., and Simon, A. (2008). "Modeling the Evolution of Incised Streams. II: Streambank Erosion." *Journal of Hydraulic Engineering, ASCE*, 134(7), 905-915.

Wood, A. L., Simon, A., Downs, P. W., and Thorne, C. R. (2001). "Bank-toe processes in incised channels: the role of apparent cohesion in the entrainment of failed bank materials." *Hydrological Processes*, 15, 39-61.

McBride, M., Hession, W. C., Rizzo, D. M., and Thompson, D. M. (2007). "The influence of riparian vegetation on near-bank turbulence: a flume experiment." *Earth Surface Processes and Landforms*, 32(13), 2019-2037.

Nepf, H. M. (1999). "Drag, turbulence, and diffusion in flow through emergent vegetation." *Water Resources Research*, 35(2), 479-489.

Niklas, K. J. (1992). “Plant Biomechanics.” University of Chicago Press, Chicago, IL.

Robert, A. (2003). “River Processes: An Introduction to Fluvial Dynamics.” Oxford University Press, New York, NY.

Schlichting, H. (1968). “Boundary Layer Theory.” McGraw-Hill, New York, NY.

Simon, A., Curini, A., Darby, S. E., and Langendoen, E. J. (2000). “Bank and near-bank processes in an incised channel.” *Geomorphology*, 35(3-4), 193-217.

Simon, A. and Collison, A. J. C. (2002). “Quantifying the mechanical and hydrologic effects of riparian vegetation on streambank stability.” *Earth Surface Processes and Landforms*, 27(5), 527-546.

Sukhodolov, A. N., and B. L. Rhoads (2001). “Field investigation of three-dimensional flow structure at stream confluences: 2. Turbulence.” *Water Resources Research*, 37(9): 2411-2424.

Tracy, H. J. and Lester, C. M., (1961). “Resistance coefficients and velocity distribution, smooth rectangular channel.” *Geological Survey Water-Supply Paper*, 1592-A. United States Government Printing Office, Washington, D.C.

Wahl, T. (2000). “WinADV Version 2.027.” U.S. Bureau of Reclamation, Water Resources Research Laboratory, Denver, CO.

White, B. L., and Nepf, H. M. (2008). “A vortex-based model of velocity and shear stress in a partially vegetated shallow channel.” *Water Resources Research*, 44(W01412), 15.

Wilkerson, G. V. (2007). “Flow through trapezoidal and rectangular channels with rigid cylinders.” *Journal of Hydraulic Engineering*, ASCE, 133(5), 521-533.

Wilson, C. A. M. E., Stoesser, T., Bates, P. D., and Batemann Pinzen, A. (2003). “Open channel flow through different forms of submerged flexible vegetation.” *Journal of Hydraulic Engineering*, ASCE, 129(11), 847-853.

Wilson, C. A. M. E., Yagci, O., Rauch, H. -P., and Stoesser, T. (2006a). “Application of the drag force approach to model the flow-interaction of natural vegetation.” *International Journal of River Basin Management*, 4(2), 137-146.

Wilson, C. A. M. E., Yagci, O., Rauch, H. -P., and Olsen, N. R. B. (2006b). "3D numerical modelling of a willow vegetated river/floodplain system." *Journal of Hydrology*, 327, 13-21.

Yalin, M. S. (1971). “Theory of Hydraulic Models.” Macmillan, London, UK.

Yang, K., Cao, S., and Knight, D. W. (2007). “Flow patterns in compound channels with vegetated floodplains.” *Journal of Hydraulic Engineering*, ASCE, 133(2), 148-159.

Zong, L., and Nepf, H. M. (2010). “Flow and deposition in and around a finite patch of vegetation.” *Geomorphology*, 116(3-4), 363-372.

Table 1. Flume and prototype scaling parameters. Hydraulic parameters are presented as means for all scenarios. The scaling factor, $\lambda$, is 4.88 for the 15° bank surface and 4.35 for the 30° bank surface. Froude scaling relations are given by Julien (2002) and Wilson et al. (2003).

| | scenario | scaling relation | model channel | prototype channel |
|---|---|---|---|---|
| Geometry | | | | |
| bank slope length | 15° | $\lambda^{-1}$ | 0.41 | 2.0 |
| (m) | 30° | $\lambda^{-1}$ | 0.46 | 2.0 |
| vertical bank face height | 15° | $\lambda^{-1}$ | 0.49 | 2.77 |
| (m) | 30° | $\lambda^{-1}$ | 0.37 | 2.77 |
| Hydraulics | | | | |
| main channel flow depth | 15° | $\lambda^{-1}$ | 0.38 | 1.85 |
| (m) | 30° | $\lambda^{-1}$ | 0.42 | 1.85 |
| cross-sectional mean velocity[1] | 15° | $\lambda^{1/2}$ | 0.19 | 0.40 |
| ($m\ s^{-1}$) | 30° | $\lambda^{1/2}$ | 0.21 | 0.47 |
| cross-sectional mean $Fr$ | 15° | $\lambda^{0}$ | 0.13-0.16 | 0.13-0.16 |
| (-) | 30° | $\lambda^{0}$ | 0.15-0.20 | 0.15-0.20 |
| Vegetation | | | | |
| stem density | 15° | $\lambda^{-2}$ | 202 | 10 |
| (stems $m^{-2}$) | 30° | $\lambda^{-2}$ | 615 | 30 |
| flexural rigidity | 15° | $\lambda^{-5}$ | 0.0435 | 120.4 |
| ($N\ m^2$) | 30° | $\lambda^{-5}$ | 0.0435 | 67.8 |
| vegetation density | $D_{lo}$ | $\lambda^{0}$ | 0.027; 0.029 | 0.027; 0.029 |
| (15°; 30° bank surface) | $D_{hi}$ | $\lambda^{0}$ | 0.085; 0.103 | 0.085; 0.103 |
| | $LD_{lo}$ | $\lambda^{0}$ | 0.155; 0.192 | 0.155; 0.192 |
| | $LD_{hi}$ | $\lambda^{0}$ | 0.468; 0.586 | 0.468; 0.586 |

[1] Velocity in the prototype channel was estimated based on the length scale factor and channel dimensions.

Table 2. Summary statistics of 64 evaluations of bank slope length and bank slope angle estimated from surveys of cross-sections 5 and 6 at the Goodwin Creek bendway, MS., established at this site in February 1996 and resurveyed at regular intervals until May 2003. The bend apex was initially at cross-section 4 and gradually migrated downstream to between cross-sections 7 and 8.

| Statistic | Bank slope length (m) | Bank slope angle (°) |
|---|---|---|
| Minimum | 1.00 | 8.8 |
| 10$^{th}$ Percentile | 1.71 | 15.7 |
| 16$^{th}$ Percentile | 1.98 | 17.3 |
| Median | 3.29 | 22.8 |
| 84$^{th}$ Percentile | 4.63 | 28.0 |
| 90$^{th}$ Percentile | 4.89 | 29.4 |
| Maximum | 5.61 | 39.8 |

Figure 1
Click here to download Figure: Figure 1.pdf

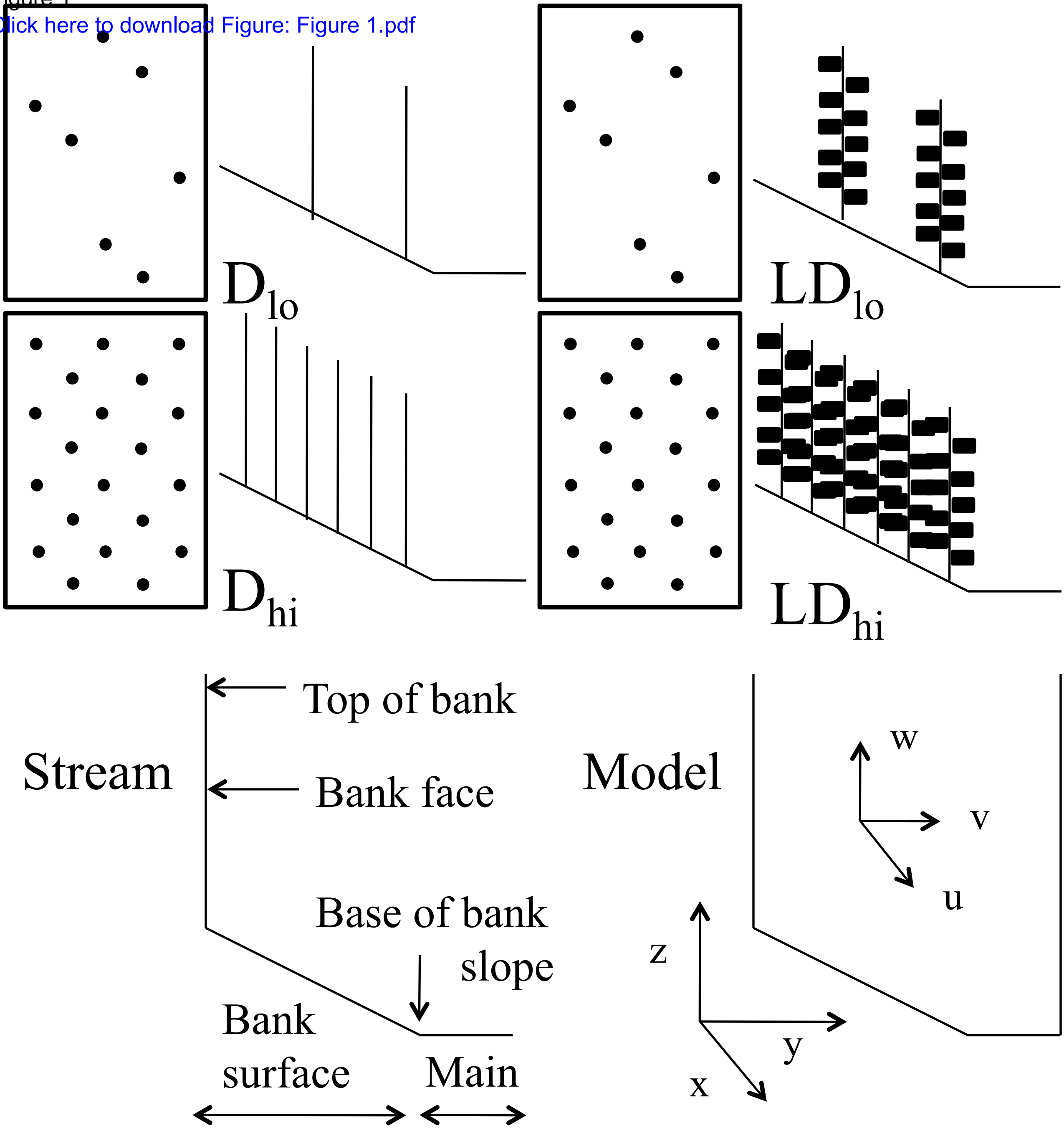

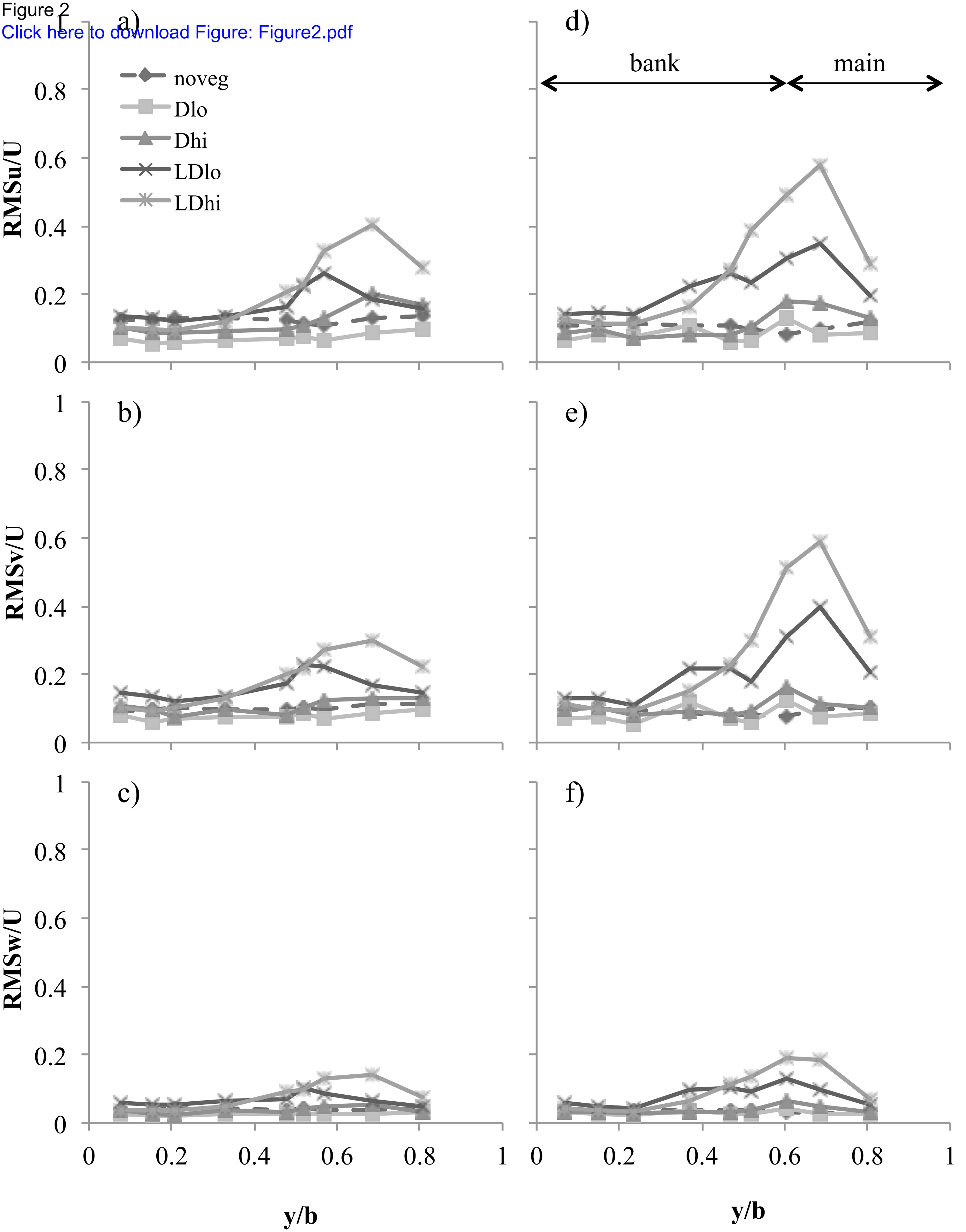
a)
b)
c)
d)
e)
f)
noveg
Dlo
Dhi
LDlo
LDhi
bank
main
RMSu/U
RMSv/U
RMSw/U
y/b
0
0.2
0.4
0.6
0.8
1

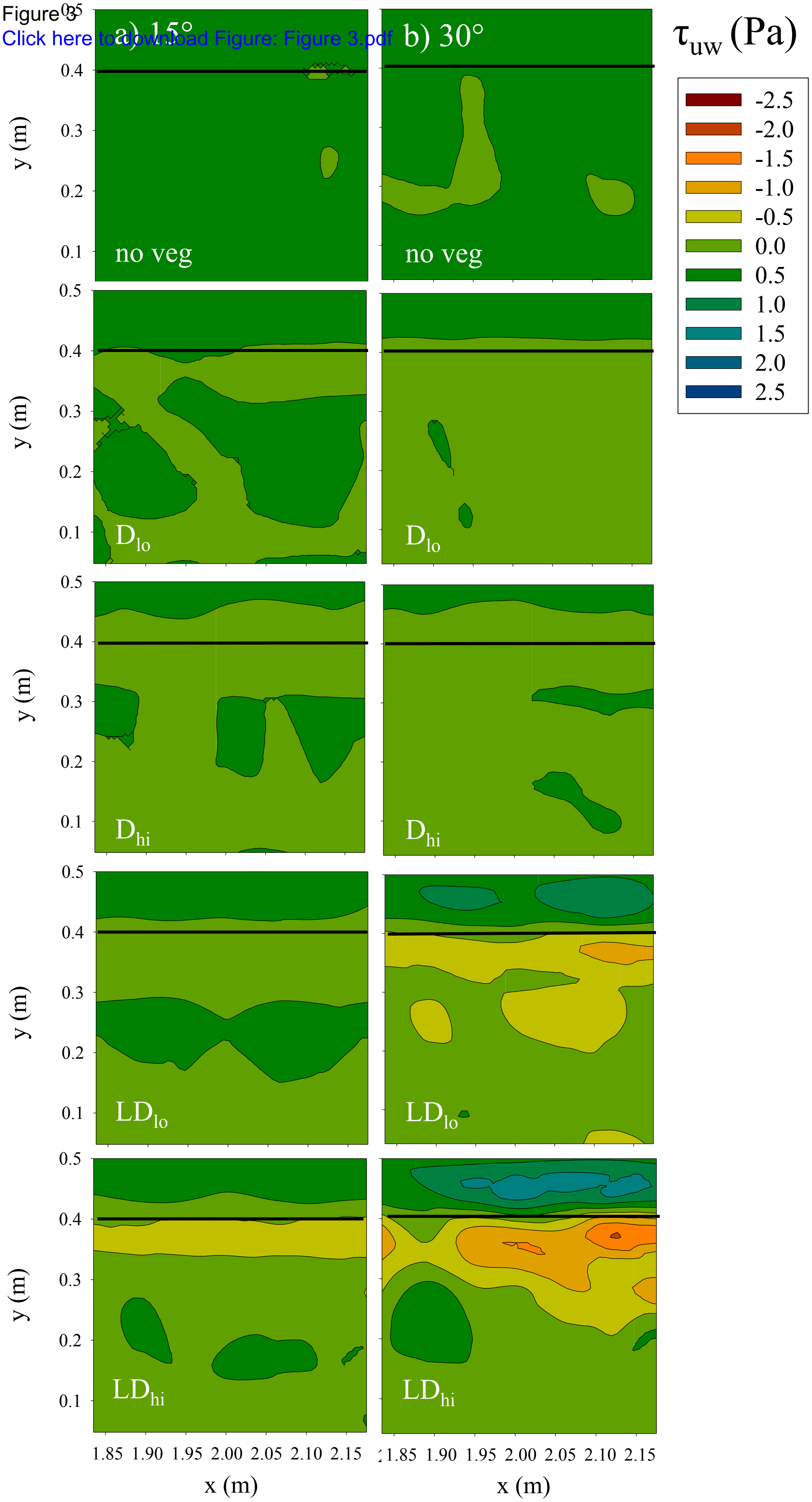
a) 15°
b) 30°
τuw (Pa)
-2.5
-2.0
-1.5
-1.0
-0.5
0.0
0.5
1.0
1.5
2.0
2.5
no veg
no veg
Dlo
Dlo
Dhi
Dhi
LDlo
LDlo
LDhi
LDhi
y (m)
0.5
0.4
0.3
0.2
0.1
1.85
1.90
1.95
2.00
2.05
2.10
2.15
x (m)

Figure 4

Click here to download Figure: Figure 4.pdf

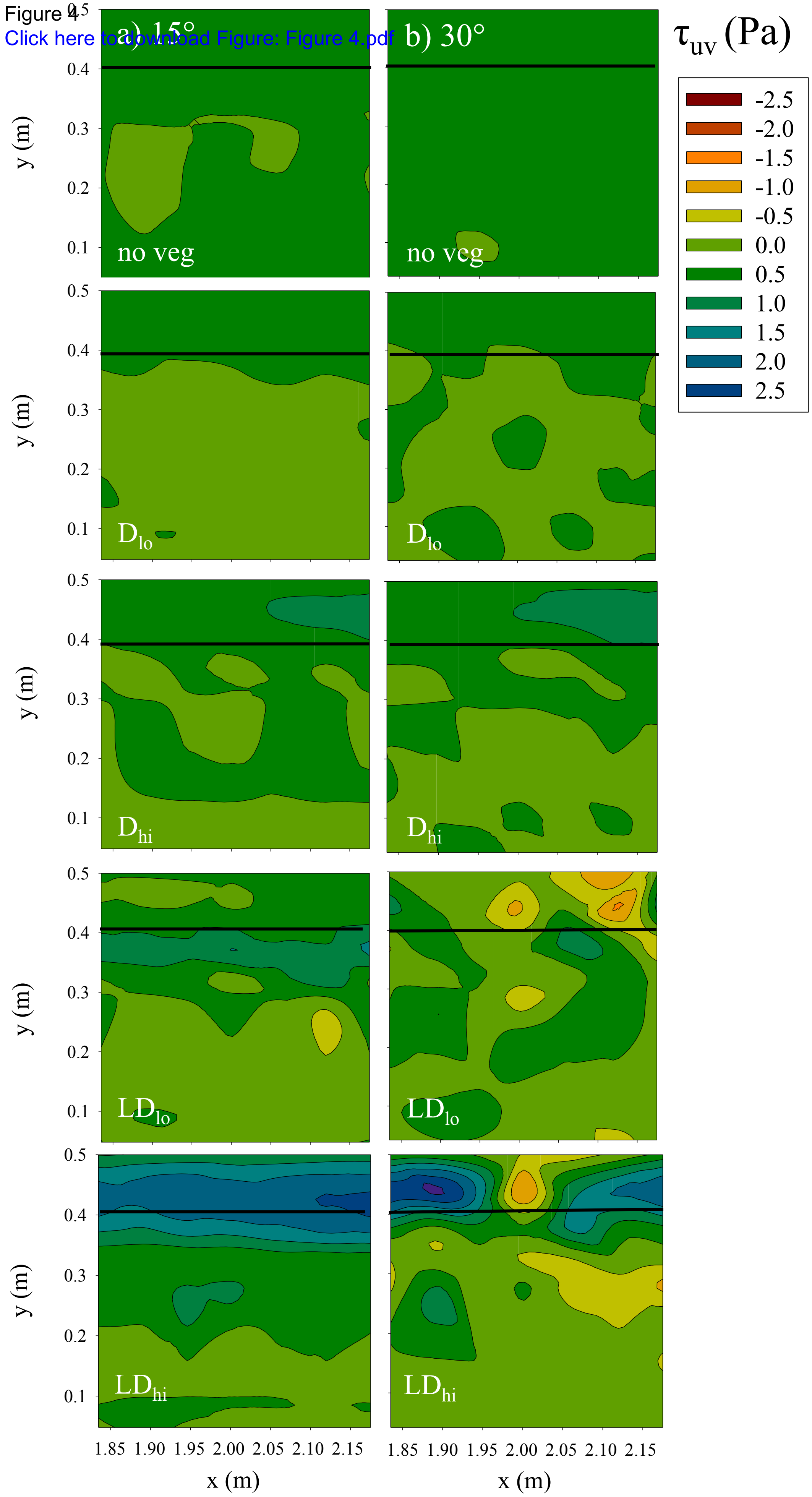

FIGURE CAPTION LIST

Figure 1. Experimental design and flume cross-sectional design. $D_{lo}$ is low density, no leaves; $D_{hi}$ is high density, no leaves; $LD_{lo}$ is low density, with leaves; and $LD_{hi}$ is high density, with leaves.

Figure 2. Cross-stream variations of near-boundary relative turbulence intensity ($RMS/U$) in the $u$ (longitudinal), $v$ (transverse), and $w$ (vertical) directions for the 15° (a, b, c) and 30° (d, e, f) bank surfaces. Velocities were measured 2.0 m downstream from the beginning of the vegetation. Cross-stream position ($y$) has been normalized by channel width ($b$). $D_{lo}$, $D_{hi}$, $LD_{lo}$ and $LD_{hi}$ are defined in Figure 1.

Figure 3. Spatial patterns of vertical Reynolds stress ($\tau_{uw}$, Pa) for the a) 15° and b) 30° bank surfaces. $D_{lo}$, $D_{hi}$, $LD_{lo}$ and $LD_{hi}$ are defined in Figure 1. The solid line represents the base of the bank slope.

Figure 4. Spatial patterns of lateral Reynolds stress ($\tau_{uv}$, Pa) for the a) 15° and b) 30° bank surfaces. $D_{lo}$, $D_{hi}$, $LD_{lo}$ and $LD_{hi}$ are defined in Figure 1. The solid line represents the base of the bank slope.